International Journal of Physics
and Research (IJPR)
ISSN(P): 2250-0030; ISSN(E): 2319-4499
Vol. 4, Issue 6, Dec 2014, 37-46
TJPRC Pvt. Ltd.

EFFECT OF INDIUM ADDITION ON THE PHYSICAL PROPERTIES OF AL-PB BEARING ALLOYS RAPIDLY QUENCHED FROM MELT

MUSTAFA KAMAL & RIZK MOSTAFA SHALABY

Department of Physics, Metal Physics Laboratory, Faculty of Science, Mansoura University, Mansoura, Egypt

ABSTRACT

In the present work, Al-5 wt. %Pb-5 wt.%In and Al-10 wt.%Pb-10 wt.%In were prepared by melt-spun technique. X-ray diffractometer, dynamic resonance method, Vickers hardness indentation and double bridge method were used to characterize the structure, mechanical, Vickers hardness and electrical resistivity of the Al_{100-x}-xPb-xIn (x=5 and 10 wt.%) alloys. Comparing the structure and mechanical properties of melt – spun Al-5Pb-5In with that of Al-10Pb-10In alloy, the effect of indium additions on structure and mechanical properties have been discussed. The present work shows that indium is an effective way of improving structure and consequently the mechanical properties of Al-Pb alloys. Also, shows that the mechanical properties of Al-5Pb-5In alloy are the best composition under the present experiment condition.

KEYWORDS: Al-Pb-In Alloy, Mechanical Properties, Hardness, Rapid Solidification

INTRODUCTION

The interest of this work is to continue and to discuss in details the aluminium monotectic melt-quenched ribbons [1, 2]. The development of immiscible alloys has been largely constrained by the conventional equilibrium processing which generally results in gross segregation due to the wide miscibility gap, and high disparity in the densities and melting temperatures between the immiscible elements [3]. For example, aluminium alloys with proper distribution of lead have potential as materials for plain bearings, because of the lubrication ability of lead in the aluminium matrix [4]. However, owing to the immiscibility of lead phase in the Al matrix [5], the grossly segregated lead may sometimes act as a kind of inclusion. Therefore, it is of importance to explore new processing approaches to obtain materials with fine distributions. During recent decades, nonequlibrium processes, such as rapid solidification and ball – milling, have been developed to produce refined controllable microstructures in immiscible systems. By means of a rapid solidification technique, Al-based (Al-In [6], Pb[7], Sn[8], Cd[9]) alloys have been synthesized with uniform distributions of the fine immiscible particles embedded in the matrix, indicating that the microstructure could be considerably refined compared with conventionally processed materials. Similar to rapid solidification is another effective nonequlibrium process for producing novel materials [10]. They reported that the synthesis of Al-Pb nanocomposites via two nonequilibrium processes, rapid solidification and ball milling, to cast light on the possibility of forming the controllable two phase mixture of Al-Pb. The microstructures as well as mechanical properties of Al-Pb samples from different approaches are analyzed and compared in the test.

Aluminium–tin alloys have good mechanical properties with conformability but these are quite costly. Lead being much cheaper than tin, leaded aluminium alloys could be very attractive alternative to Al–Sn bearing materials [11-14]. It is well known that lead is more effective than tin as a soft phase alloying addition which confers the necessary anti scoring and antifrictional properties [14, 15], with low wear [16]. A low modulus of elasticity [11] is required in a bearing

alloy to ensure good compatibility with the journal surface. Aluminium has a low modulus of elasticity and apart from indium, lead has the lowest modulus of elasticity of all the soft phases alloying with aluminium [17]. It has also been reported [14, 16, 18] that Al–Pb alloys are attractive and cheaper alternative to the commonly employed Al–Sn bearing alloys. However, preparation [18-20] of Al–Pb alloys is difficult due to solid insolubility of lead in aluminium and vice versa. Wide miscibility gap in liquid state along with higher density difference and large solidification range make the alloys preparation very difficult. But attractive bearing properties [15, 21-25] of Al–Pb alloys emphasized the need to develop these alloys for the substitution of conventional bearing alloys, particularly, aluminium– tin.

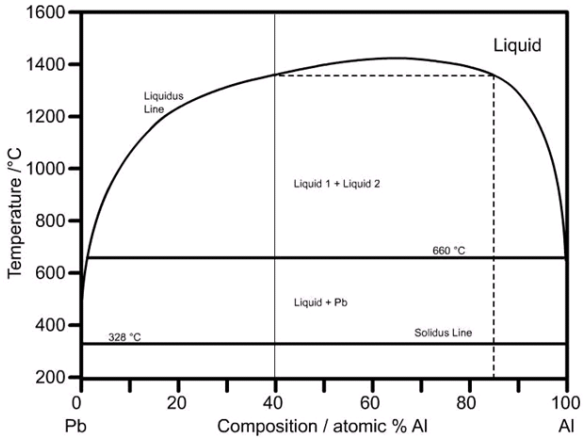

Figure 1: Phase Equilibrium of Al-Pb Monotectic Alloy

The simple monotectic phase equilibrium of Al-Pb, Figure 1, shows that negligible solubility in the solid-solid and solid-liquid domains have been aimed at a better understanding of nucleation phenomena associated with melting and freezing of small confined particles. The solidification studies of immiscible alloy systems such as Al-Bi, Al-Sn, Al-Pb, Al-Si-Pb, Al-Pb-Si etc. is important from scientific and technical point of view [26-28]. The Al-Sn and Al-Pb based alloys have been commonly accepted for having excellent tribological and mechanical properties. These kinds of alloy system are suitable for engineering applications, particularly self-lubrication bearing materials. Owing to the lower solubility, the parent liquid is decomposed into two distinct immiscible liquid phases when it passes through the immiscibility gap, and then followed by severe segregation due to the large density difference between two different density liquid phases. In Al-Sn and Al-Pb alloy systems, phase separation occur when the Sn and Pb content are higher than 0.09 wt.% and 0.2 wt.%, respectively. To overcome segregation problem in immiscible alloy many methods have been proposed, such as stir casting, ultrasonic, the casting and rapid solidification. Al-Pb monoetectic alloys with different compositions were rapidly solidified from melt using chill-block melt-spin technique have been studied by [2]. The results showed that the structures of all melt-spun ribbons were completely composed two distinct phases of aluminium rich phase and lead rich phase. The results also show that this material is very sensitive to the compositions. Recently, Fan *et. al* [29] developed a melt conditioning advanced shearing technology (MCAST) device to create a fine and homogeneous liquid dispersion within the miscibility gap and then the viscous force offered by semi-solid slurry to counterbalance the gravity force and the Marangoni effect [30, 31]. Lian-Yichen et al [32] reported the rapid control of phase growth by nano particles, the effectiveness of this approach is demonstrated in both inorganic (immiscible alloy and eutectic alloy) and organic material their approach overcomes the microstructure refinement limit set by the fast phase growth during cooling and breaks the inherent limitations of surfactants for growth control. The aim of this investigation was to develop cheaper substitutes for the common but expensive bearing alloys, particularly, aluminium–tin alloys. To this end an attempt has

been made to develop leaded aluminium (Al-Pb-In) alloys which possess equivalent bearing property to that of conventional aluminium–tin alloys.

EXPERIMENTAL DETAILS

The Al_{100-x}-Pb_x-In_x (x=5 and 10 wt. %) immiscible alloys were prepared from commercial pure aluminium with appropriate addition of 99.99 wt.% pure Pb and In. The melt was prepared in a porcelain crucible in an electric resistance furnace. The furnace temperature was gradually increased and held 900 °C to homogenize the melt. The Al-Pb-In thin ribbons 3-6 mm wide, 60-100 μm thick, and a few meters long were obtained by using the melt-spinning technique. The melt spinning Al-Pb-In samples were examined by using x-ray diffraction (XRD), with the Cu K_α radiation. The average grain sizes and lattice parameters were determined, respectively, by means of quantitative analysis of the XRD spectra. Microhardness was measured in an H_v microhardness tester at a load of 25 gf, for which the melt spun ribbons. At least ten measurements for each sample were collected to calculate the average values.

RESULTS AND DISCUSSIONS

Structure

Figure 1 shows the X-ray diffraction patterns for as-quenched melt-spun Al-5Pb-5In and Al-10Pb-10In alloys. All the recorded diffraction peaks at the same value of 2θ, for Al-5Pb-5In alloy, Figure 1a denoting the presence of lead, aluminium and indium with F.C.C. and tetragonal structure. (JCPDS Data file: 04-646, 04-787, and 05-642) respectively. The pattern for Al-10Pb-10In alloy, Figure 1b shows the same phases with decreasing the intensity of the X-ray diffraction peaks but with increasing of no. of Pb peaks from one to four peaks, on the other side, the No. of indium peaks decreasing from five to two peaks. This means that decreasing the solubility of Pb but increasing the solubility of indium in Al matrix. The solubility of Pb and In in Al matrix causes a small shift of the x-ray diffraction peaks to higher angle. This shift may be attributed to the higher atomic radius of lead atoms compared to Al atoms. It can be observed that there is a shift in Bragg angles at which diffraction occurred and also broadening of the base took place. The details of the XRD analysis are listed in Table 1. The lattice parameters of aluminium phase increased steadily with increasing alloying content as shown in Table 1 reaching a value of 4.1095 Å for Al-10Pb-10In alloy. The increase in the lattice parameter of aluminium phase with lead indicates that the amount of dissolved indium has increased. So it is, an important results in our case indicating that the melt spinning technique enhanced the solubility limit of indium in aluminium as a good material used in bearing applications [33, 34]. The next step after identifying the phases of the unit cell is to find the number of atom in the unit cell. To find this number we use the fact that the volume of the unit cell calculated from the lattice parameters multiplied by the measured density, ρ, of the melt-spun ribbons equals the weight of the all the atoms in the cell, for any crystal [35]:

ρ = weight of atoms in unit cell / volume of unit cell

Or

$$\rho = \frac{\sum A}{NV} \qquad 1$$

If V in equation 1 for the density of a crystal is expressed in A^3 and the currently accepted value of Avogadro's number N inserted, then the equation [1] becomes

$$\sum A = \frac{\rho V}{1.6602} \quad (2)$$

$$\sum A = nA \quad (3)$$

Where n is the number of atoms per unit cell and A is the atomic weight. Results for the number of atoms per unit cell of the Al-phase in melt- spun Al-Pb-In alloys are listed in Table 2. The number of atoms per unit cell in any crystal is partially dependent on its Bravais lattice. So when determined in this way, the number of atoms per cell is always an integer such as in the bulk sample of aluminium pure, within experimental error, except for some which have defect structures. In our case melt-spun ribbons, atoms are simply missing from a certain fraction of these lattice sites which they would be expected to occupy, and the result as shown in Table 2 is a non-integral number of atoms per cell. The value of the measured density for Al-5Pb-5In and Al-10Pb-10In rapidly solidified are 2.34 and 2.43 gm/cm^3 respectively as shown in Table 2. Also, the number of the atoms per unit cell 3.5 and 3.6 for two alloys, which must be 4 for Al. Therefore, some of the atoms may be missing from a certain fraction of those lattice sites that they would be expected to occupy. The apparent crystal size of Al, Pb and In are refined. The apparent grain size of Al and Pb was calculated using the Scherer equation $D_{hkl} = 0.9\lambda / \beta_{hkl} \cos\theta$, where D_{hkl} is the grain size, λ is the wavelength of Cu Kα = 1.54056 Å, θ is the reflection angle and βhkl is the full width at half maximum (FWHM) [36]. Table 2 displays the average crystal sizes of Al and Pb, which were determined respectively, from the half-maximum width of the Pb(111), (200), and Al (111) diffraction peaks, as a function of particle size. The particle size and the volume of unit cell of the α-Al matrix were calculated from XRD, and the results are shown in Table 1. It was found that the alloy containing 5 wt.% In has the smallest particle size and the largest volume of the cubic unit cell of the α-Al matrix.

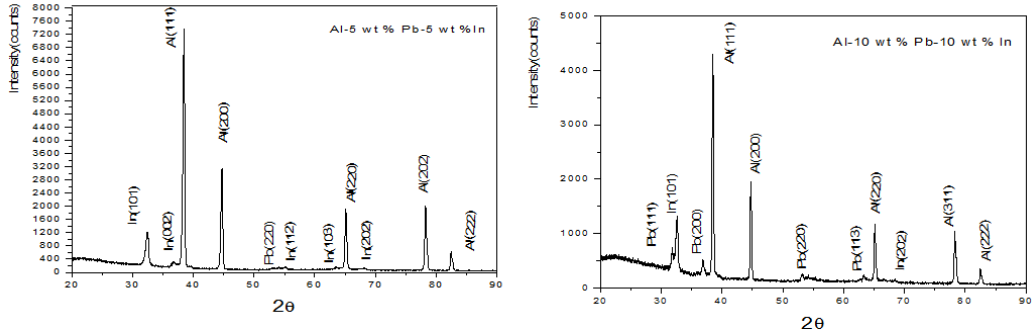

Figure 1: The X-Ray Diffraction Patterns Using Cu K$^{\alpha}$ and its Analysis of Ternary (a) Al-5 Wt % Pb-5 Wt % in, (b) Al-10 Wt % Pb-10 Wt % in Rapidly Solidified Ribbons

Table 1: The Structure of Phases Present in the A-Al Matrix

System	Phases Present	Crystal System	No. of Peaks		Lattice Parameter (A)	
				a	c	c/a
Al-5 wt.% Pb-5 wt.%In	α-Al Pb In	Face centerd cubic Face centerd cubic tetragonal	5 1 5	4.0501 4.8795 3.240	4.9017	1.510
Al-10 wt.% Pb-10 wt.% In	α-Al Pb In	Face centerd cubic Face centerd cubic tetragonal	5 4 2	4.0514 4.8674 3.2300	4.8975	1.516

Table 2: Determination of the Number of Atoms of Al Phase in a Unit Cell

System	Number of Atoms / Unit Cell	Lattice Parameter of Al Phase (Å)	Volume of the Unit Cell (Å ^{3})	Density (Gm.Cm^{-3})	Graim Size (µm)
Al-5 wt % Pb-5 wt % In	3.5	4.0501	66.5	2.34	312.6
Al-10 wt % Pb-10 wt % In	3.6	4.0514	66.4	2.43	553.6

Mcrohardness Indentation and Yield Stress

Hardness measurements can be used to obtain yield stresses for melt-spun ribbons used in this study and to estimate impact yield stresses [37]. The maximum shear stress that is created by a locally applied pressure occurs on the central axis below the pressurized region as indicated by Timoshenko and Goodier [38]. The maximum shear stress will be

$$\tau_m = 0.5H\{\frac{1}{2}(1-2\upsilon)+0.22(1+\upsilon)[2(1+\upsilon)]^{\frac{1}{2}}\} \quad 4$$

Where, υ is the Poisson's ratio. The values of τ_m for Al-5Pb-5In and Al-10Pb-10In melt-spun ribbons are listed in Table 3.

Table 3 shows the microhardness of the melt-spun Al-Pb-In alloys as a function of indium content. Several features can be noticed from Table 3. Firstly, the microhardness of the melt-spun Al-10Pb-10In sample is much larger than that of the Al-5Pb-5In sample. In fact, the microhardness of the Al-Pb samples increased gradually with the refinement of both Al, Pb and In components. It has been experimentally observed that, in conventional materials, the hardness varies with the grain size following the empirical Hall-Petch relation:

$H_v=\sigma_0 + K_0 d^{-1/2}$, where H_v is the hardness, σ_0 is the intrinsic resisting distribution motion, k_0 is a constant, and d is the grain size. In the present work, although melt spun Al-Pb-In alloys are three phase mixtures; their considerably increased hardness might be attributed to the refinement of the main Al component in the melt spun sample according to the Hall-Petch relation. Secondly, one may find from Table 3, that there is a maximum microhardness value corresponding to a Pb content of 10 wt. % for both samples. Since the grain size of the Al matrix in either the Al-10Pb-10In or the Al-5Pb-5In samples are nearly small value, variation of the Vickers hardness might be caused by the addition of lead and indium. Because of their fine-scale dimension, lead nanoparticles might act as a kind of strengthening particles rather than coarse inclusions. The dispersed Pb particles are weaker than the Al matrix; they will be shared by the gliding dislocations, which imply the dislocation motion, and thus strengthens the Pb dispersed composites, causing the microhardness increases. One can argue that the strengthening effect from Pb nanoparticles depends on their volume fractions as well as particle sizes. A small amount of the fine Pb particles will effectively strengthen the melt spun Al-Pb; the microhardness will increase with the addition of the Pb, when the content of Pb is greater than such a critical value (5 wt.%), which actually corresponds to its critical volume fraction or particle size, the softer large Pb particles will play a role in weakening the Al-Pb alloys, as shown in Table 3 that the Vickers hardness decrease when the content of Pb is greater than 5 wt.%.

Table 3: Microhardness Indentation (HV), Maximum Shear Stress and Friction

System	HV (MPA)	Maximum Shear Stress (MPA)	Friction (10^{-2}) ($T_{m/H}$)
Al-5 wt %Pb-5 wt % In	469.7	87.5	18.6
Al-10 wt % Pb-10 wt % In	493.9	112.6	22.8

Internal Friction and Dynamic Young's Modulus

The strength of the material is limited by the atomic bonding forces, which are reflected macroscopically by the elastic constants. Table 4 shows the values of the elastic moduli of all prepared alloys calculated from the resonance curve obtained by the dynamic resonance circuit after determination of the resonance frequency. The Young's modulus showed an appreciable increase from 21 GPa for Al-10Pb-10In to 30 Gpa for Al-5Pb-5In. It shows an increase of the elastic modulus to the maximum value of 30 GPa at 5 wt. % In. At first the value of E for Al-5Pb-5In rapidly solidified was found to be 30 GPa. On the addition of Pb at 10 wt. % to Al, the value of E increases to a maximum value 21.8 GPa as presented. This increase may be explained as due to the presence of hard α-phase which acts as hard inclusions in the soft matrix as outlined above. Also, this observed behavior of young's modulus can be explained in terms of the variation in the volume of the unit cell of Al matrix. Values of bulk modulus (K) and shear modulus (G) were calculated using standard equations:

$$K=E/3(1-2\upsilon),\ G=E/2(1+\upsilon) \qquad 5$$

Where E is the Young's modulus and υ is the Poisson's ratio. The trend in developing new bearing alloys can be viewed as the opportunity to improve device performance and reliability. The interesting trend in this field is that high mechanical strength combined with good ductility tends to increase fatigue life. Measured values are listed in Table 4, for the constant of proportionality between stress and strain is called a modulus of elasticity.

The measured internal friction, Q^{-1}, as a function of composition are listed in Table 4. It is seen that the internal friction is sensitive to the content of in and Pb as alloying elements to Al metal as indicated in Table 4. It is clear that the internal friction, Q^{-1}, decreased with the addition of Pb at 10 wt.%, this may be explained by a reduction in transformable shear stress with the largest free volume. Also, the increase in the internal friction is due to the motion of substitutional indium atoms in Al crystals, since the presence of vacancies facilitates the motion of the indium atoms. The problem of understanding the intrinsic an elastic behavior of melt-spun ribbons of Al-Pb-In immiscible alloys by dynamic resonance method is not unequivocal clear cut. There are some reasons for that: the melt spun ribbons prepared by melt spinning technique, the results are affected by extrinsic structural parameters, such as the porosity, the melting temperature and the densification behavior of Al-Pb-In alloys. A low level of Q^{-1} for Al-10Pb-10In rapidly solidified from melt implies a rigid structure which may be due to the absence of the locking of crystal defects [39].

Table 4: Mechanical Properties and Internal Friction (Q^{-1}) of Melt Spun $al_{(100-X)}$-Pb_x-In_x (X=5, 10) Alloys

System	E (G Pa)	G (G Pa)	K (G Pa)	Q^{-1} ($\times 10^{-4}$)	Poisson's Ratio
Al-5 wt % Pb-5 wt % In	30.00	11.00	35.70	337.00	0.360
Al-10 wt % Pb-10 wt % In	21.80	7.90	27.70	329.00	0.369

Thermal Diffusivity and Electrical Conductivity

Thermal diffusivity is a term useful in dealing with heat flow and it's defined by the equation $D_{th}=k/C\rho$ where k is the thermal conductivity, C is the heat capacity and ρ is the density. So this property gives an better indication of the way in which a material responds to transient thermal stimuli. Anyhow, the high diffusivity is of utmost importance in

explaining many aging phenomena for example unattenuated high rates of crystal growth and the wide spread in a activation energies for crystallization.

The linear law relating heat flow and temperature gradient gives only a partial description of the thermal processes involved in solids. This can be expresses in terms of the Fourier's law U=-λ gradT, Where U is the heat current, λ thermal conductivity, T absolute temperature and the minus sign arises from the fact that heat always flows from the hotter to the colder region. The changes in internal energy can be expressed in terms of the specific heat C multiplied by the density ρ

$$C\rho\, dT/dt = -divU = div\,(\lambda\, gradT) \quad (6)$$

Where t is time the form of this equation allows for the possibility of the thermal conductivity varying with position, either owing to the temperature gradient or to actual in homogeneity of the result-spun ribbons used. So the equation [6] is written

$$dT/dt = D_{th}\, \nabla^2\, t \quad (7)$$

Where D_{th} is the thermal diffusivity.

The values of thermal diffusivity D_{th}, of Al-5Pb-5In and Al-10Pb-10In melt spun ribbons controls the time rate at which the melt-spun ribbons with a non uniform temperature reaches a state of thermal equilibrium. The mathematical formula that relates thermal diffusivity D_{th} to the resonance frequency f_0 at which the peak damping occurs using the dynamic resonance method [40] is

$$D_{th} = 2d^2 f_0/\pi \quad (8)$$

Where d is the thickness of the ribbon. The specific heat, C of the ribbons can be expressed in terms of the resonance frequency f_0 and the thickness of the ribbons d, by introducing equation of thermal diffusivity in equation 8 we have

$$2d^2 f_0/\pi = k/C\rho \quad (9)$$

The thermal conductivity of the melt-spun ribbons of the samples used in this study can be expressed in terms of the electrical conductivity using the modified Wiedman-Franz ratio [41, 42];

$$k = 5.02\delta T \times 10^{-9} + 0.03 \quad (10)$$

Where δ is the electrical conductivity and T is absolute temperature. The thermal diffusivity and the electrical conductivity of melt-spun ribbons of Al-5Pb-5In and Al-10Pb-10In as a function of Indium content are depicted in Table 5. A nonlinear increase of thermal diffusivities with an increase in lead content is observed in all case. It is assumed that this fact is caused by some aggregation of lead particles, particularly the distribution of lead particles is important in determining the effective spreading of lead in forming a layer of solid lubricating, while employed in a bearing. Thermal diffusivity values and electrical resistivity for alloys are illustrated in Table 5. The maximum value of thermal diffusivity calculated for Al-5Pb-5In alloy might due to the presence of the soft phases α-Al, Pb and In. Generally, the thermal diffusivity values are lower for the melt-spun alloys whose internal friction was higher. This might be due to the depression of defects by the melt spun process during the preparation. The electrical resistivity (ρ) of as-quenched melt spun Al-5Pb-5In and Al-10Pb-10In alloys were measured, and the result is shown in Table 5. The electrical conductivity was increased by the addition of indium up to maximum value 795.5 ohm.m at 5 wt. % In, compared with 489.5 ohm. m for

Al-10Pb-10In alloy.

Table 5: Thermal Diffusivity, Specific Heat, Thermal Conductivity and Electrical Conductivity of $Al_{(100-X)}$-Pb_x-In_x (X=5, 10) Alloys

System	Thermal Diffusivity (10^{-10} $M^2.Sec^{-1}$)	Specific Heat (10^8j/Kg.°C)	Thermal Conductivity ($W \cdot M^{-1} \cdot K^{-1}$)	Electrical Conductivity ($10^4 \Omega^{-1}.M^{-1}$)
Al-5 wt % Pb-5 wt % In	10	49.6	11.6	795.5
Al-10 wt % Pb-10 wt % In	13	23.5	7.42	489.5

CONCLUSIONS

The present study investigations reflect the influence of Indium addition on Structure and mechanical properties of Al-Pb rapidly solidified alloys. Also, the study concludes that melt-spun technique is an effective technique for producing a uniform dispersion of indium droplets in aluminium- lead monotectic alloys. The particle size in the aluminium phase become slightly smaller as the indium addition increased in the Al-Pb monotectic alloys. It also concluded that measured values of the elastic moduli and internal friction affect by indium addition. It is found that the distribution of indium and lead particles is important in determining the effective spreading in forming a layer of solid lubricating, while employed in bearing. Generally, it is concluded that the liquid-liquid disintegration can be initiated by a series of acts of nucleation of the second liquid phase in Al-Pb monotectic liquids

REFERENCES

1. Mustafa Kamal, A. B. El-Bediwi and Mohamed Majeed Hameed, IJET-IJENS, Vol: 1, No.04 (2014)23-32.
2. Mustafa Kamal, A. b. El-Bediwi and Samira El-Mohamady Fouda, IJET-IJENS, Vol: 13, No.06 (2013)29-38.
3. A. N. Patel and S. Diamond, Mater. Sci. Eng., 98, (1988) 329.
4. J. P. Pathak, V. Singh, and S. N. Tiwari, J. Mater. Sci. Lett. 11, (1992), 639.
5. T. B. Massalki, Binary Alloy Phase Diagrams (American Society for Metals, Metals Park, OH, 1986).
6. H. Saka, Y. Nishikawa, and T. Imura, Philos. Mag. A 57, (1988), 89.
7. D. L. Zhang and B. Cantor, Acta Metall. Mater. 39, (1991), 1595.
8. W. T. Kim and B. Cantor, J. Mater. Sci. 26, (1991), 2869.
9. D. L. Zhang, J. L. Hutchinson, and B. Cantor, J. Mater. Sci. 29, (1994), 2147.
10. C. C. Koch, Mater. Tran. JIM 36, (1995), 85.
11. Dayton R W, Sleeve bearing materials (Cleveland, Ohio: ASM), (1949), 6.
12. Wonderwood A F, Sleeve bearing materials (Cleveland, Ohio: ASM), 1949, p. 210.
13. Forrester P G, *Met. Rev.* 5 (1960), 507.
14. Tiwari S N, Pathak J P and Malhotra S L, Aluminium 4 (1987), 3.
15. Geng H and Ma J, *Wear* 169(1993), 201.

16. Pathak J P, Tiwari S N and Malhotra S L, *Wear* 112 (1986), 341.
17. Tegart W I M, Elements of mechanical metallurgy (New York: The MacMillan Co.) (1966), 91.
18. Borogunov V G, Parshin V D and Panin V V, Russ. Cast Prod. (1973), 353.
19. Pathak J P, Tiwari S N and Malhotra S L, Metals Tech. 6 (1979), 442.
20. Ratke L, Zao J Z and Dree S, Mater. Sci. & Eng. A282, (2000), 262.
21. Hodes E and Steeg M, Flugwiss Weltraumforsch 2 (1978), 337.
22. Tiwari S N, Pathak J P and Malhotra S L, Metals Technol.10 (1983), 413.
23. Pathak J P and Tiwari S N, Aluminium Indian 7 (1990), 3.
24. Hove D P, Mee M, Torrance A A and Williams J D, Mater. Sci. & Technol. 7 (1991), 330.
25. Pathak J P, Torabian H and Tiwari S N, Cast Metals 7 (1995), 201.Pratt G C, Int. Met. Rev. 18(1973), 62.
26. L. Ratke and S. Diefenbach, “Liquid immiscible alloys,” Mater. Sci. and Eng., R15 (1995), 263-347.
27. L. Ratke: Immiscible liquid metals and organic (The proceeding of immiscible alloys, Physikzentrum, Bad Honnef 1992).
28. J. Z. Zhao and L. Ratke, Scripta Materialia, 50(2004), 543-546.
29. Z. Fan, S. Ji, and J. Zhang, Mater. Sci. Tech., 17 (2001), 837-841
30. D. Mirkovi´c, J. Gr¨obner, and R. Schmid-Fetzer, Mater. Sci. and Eng., 1-2(2008), 456-467.
31. X. Fang and Z. Fan,, Scripta Materialia, 54 (2006), 789–793.
32. Lian-Yi Chen, Jia Quan Xu, Hongseok Choi, Hiromi Konishi, Song Jin and Xiao-Chun Li, Nature Communications 5, [no.5: 3879], 09 may 2014, 1-9, Macmillan publishers limited.
33. Ch. v. S. H. S. R. sastry, and G. Range Janardhana, Indian Journal of Engineering & materials sciences, vol.17, February (2010) 56-60.
34. H. R. Kotadia, J. B. Patel, Z. Fan, E. Doernberg, and R. Schmid-Fetzer, TMS (The Minerals, Metals & Materials Society), 2009, pp:81-88 G.Korekt and L.Ratke, Materials Science Forum, Vols. 215-216 (1996) 81-88.
35. Mustafa Kamal, Shalabia Badr and Nermin Ali Abdelhakim, IJET-IJENS, 14 (2014)119-129.
36. B. D. Cullity, Elements of X-ray Diffraction, 2nd edition, Addision-Wesely, 1978, p.248.
37. J. J. Gilman, Journal of Applied Physics, Vol. 46, No. 4, April (1975) 1435.
38. S. Timoshenko and J. Coodier, Theory of Elasticity, 3 rd Ed. Mc Graw – Hill, New York, (1970), 407.
39. E. Bonetti, L. Del Bianco, L. Pasquini, and E. Sampaolesi, nanostructured Materials, Vol.10, No.5. (1998) 741-753.
40. Mustafa Kamal and El-Said Gouda, Radiation Effects & Defects in Solids, Vol. 162, No. 9, September (2007) 691-696.

41. Mustafa Kamal and Abu-Bakr El-Bediwi, Radiation Effects & Defects in Solids, November – December, 159 (2004) 651-657.

42. G. E. Doan, The principles of Physical Metallurgy, 3 rd. ed, McGraw Hill Book Company, New York (1953).